

The Involvement of Hydrogen-producing and ATP-dependent NADPH-consuming Pathways in Setting the Redox Poise in the Chloroplast of *Chlamydomonas reinhardtii* in Anoxia

Received for publication, December 13, 2014, and in revised form, February 4, 2015. Published, JBC Papers in Press, February 17, 2015, DOI 10.1074/jbc.M114.632588

Sophie Clowez^{†1,2}, Damien Godaux^{§3}, Pierre Cardol^{§3,4}, Francis-André Wollman^{†2}, and Fabrice Rappaport^{†2,5}

From the [†]Institut de Biologie Physico-Chimique, UMR 7141 CNRS-UPMC, 13 Rue P et M Curie, 75005 Paris, France, and the [§]Laboratoire de Génétique et Physiologie des Microalgues, Phytosystems, Department of Life Sciences, Institute of Botany, 27 Bld. du Rectorat, University of Liège, B-4000 Liège, Belgium

Background: Shift to anoxia promotes the over-reduction of photosystem I electron acceptors.

Results: This over-reduction can be relieved by the activation of several pathways.

Conclusion: The two main pathways are the ATP-dependent CO₂ fixation pathway and the ATP-independent hydrogenase.

Significance: We disentangle the role of the various NADPH-consuming pathways in setting the redox poise in the chloroplast of unicellular photosynthetic algae.

Photosynthetic microalgae are exposed to changing environmental conditions. In particular, microbes found in ponds or soils often face hypoxia or even anoxia, and this severely impacts their physiology. *Chlamydomonas reinhardtii* is one among such photosynthetic microorganisms recognized for its unusual wealth of fermentative pathways and the extensive remodeling of its metabolism upon the switch to anaerobic conditions. As regards the photosynthetic electron transfer, this remodeling encompasses a strong limitation of the electron flow downstream of photosystem I. Here, we further characterize the origin of this limitation. We show that it stems from the strong reducing pressure that builds up upon the onset of anoxia, and this pressure can be relieved either by the light-induced synthesis of ATP, which promotes the consumption of reducing equivalents, or by the progressive activation of the hydrogenase pathway, which provides an electron transfer pathway alternative to the CO₂ fixation cycle.

The natural habitat of many photosynthetic microalgae, such as *Chlamydomonas reinhardtii*, exposes them to changing environmental conditions. The first conditions that come to mind are fluctuations in light intensity, but hypoxia or even anoxia is also frequently encountered by photosynthetic microbes found in soils or ponds, a biotope they usually share with dense microbial communities comprising nonphotosynthetic organisms who actively consume oxygen as they respire (1). *Chlamydomonas reinhardtii* is remarkably equipped with a battery of fermentative pathways allowing it to metabolize

pyruvate into lactate or even ethanol, formate, acetate, and hydrogen (2–5). The transition from aerobiosis to hypoxia or anoxia, which occurs in natural habitat at twilight and at night when photosynthetic oxygen evolution switches off, is accompanied by a massive metabolic remodeling that involves transcriptional regulation and the onset of dedicated metabolic pathways (6–10), and prominent among them is, in *C. reinhardtii*, the hydrogen production pathway (2, 11).

In addition to the activation of these specific pathways, anoxia strongly impacts the chloroplast. The sudden shortage of ATP resulting from the combined arrest of the photosynthetic electron transfer chain in the dark and of the mitochondrial one promotes, through the so-called Pasteur effect, the activation of the glycolytic pathway (12, 13) that produces not only ATP but also NADPH, which, at least transiently, builds up because of the lack of terminal electron acceptor to drive its consumption. This increased intra-chloroplastic reducing power is witnessed by the progressive reduction of the plastoquinone pool promoted by the dehydrogenase Nda2 (14) which, in hypoxia, outcompetes the plastid oxidase PTOX2 (15). In *C. reinhardtii*, this, in turn, induces a massive ultrastructural reorganization of the thylakoid through a process known as State Transition (16, 17), by which the mobile light-harvesting proteins LHCI are phosphorylated (18), disconnected from photosystem II, and transferred to the non-appressed stroma lamellae where they become associated with photosystem I (19–22). This ultrastructural change has long been thought to be intimately linked with another essential functional adjustment, the switch from linear (LEF)⁶ to cyclic electron transfer (CEF) (23, 24). However, the causality link between these two transitions has been recently disproved (25, 26), and they both have been shown to be independent even while being triggered by the increased reducing pressure (26–29). It remains however that the switch from LEF to CEF is associated with another ultrastructural change than the lateral

¹ Recipient of a Ph.D. fellowship from Université Pierre et Marie Curie.

² Supported by CNRS and the “Initiative d’Excellence” Program from French State Grant “DYNAMO,” ANR-11-LABX-0011-01.

³ Supported by the Belgian Fonds de la Recherche Scientifique-Fonds National de la Recherche Fondamentale Collective Grant 2.4597.11 and Mandat d’Impulsion Scientifique Grant F.4520.

⁴ Research Associate from Fonds de la Recherche Scientifique-Fonds National de la Recherche Scientifique.

⁵ To whom correspondence should be addressed. Tel.: 33-1-58-41-50-59; Fax: 33-1-58-415-022; E-mail: Fabrice.Rappaport@ibpc.fr.

⁶ The abbreviations used are: LEF, linear electron transfer; PSI, photosystem I; PSII, photosystem II; CEF, cyclic electron transfer; Rubisco, ribulose-bisphosphate carboxylase/oxygenase; DCMU, 3-(3,4-dichlorophenyl)-1,1-dimethylurea.

redistribution of LHCII, *i.e.* the formation of supercomplexes clustering in a single biochemical entity, including most of the actors of CEF (25, 26, 30), and nicely correlating, so far, with the enhancement of CEF.

Recently, we (26) and others (29, 31) reported that upon the switch from oxic to anoxic conditions, the increase in reducing pressure is such that PSI undergoes an acceptor side limitation, as defined in Ref. 32, that is pronounced enough to prevent almost completely the light-induced oxidation of PSI (29). In addition to this, we observed, consistent with the findings of Ghysels *et al.* (31), that this acceptor side limitation is spontaneously alleviated upon incubation in anoxic conditions for about 40 min (26). This spontaneous evolution is likely another facet of the metabolic remodeling described above, but its molecular or enzymatic determinants remain uncharacterized. Yet, the transition from darkness to light of photosynthetic cells adapted to anoxia is of physiological relevance as it likely set the tone for the reactivation of photosynthesis in natural conditions. Here, we address this issue by using several *C. reinhardtii* mutants affected in the pathways that make good candidates for being responsible for the spontaneous or the light-induced alleviation of the PSI acceptor side limitation. We thus support the hydrogenase enzyme as being the main player in the ATP-independent adjustment of the stromal redox poise during incubation in anoxia (31). Moreover, we show that, as expected, in the absence of linear electron flow the PSI-cyclic electron flow promotes synthesis of ATP and in turn the activation of the ATP-dependent NADPH-consuming pathways, thereby facilitating the reactivation of the photosynthetic electron flux.

EXPERIMENTAL PROCEDURES

Strains and Growth Conditions—We used the following *C. reinhardtii* wild-type strain T222+, the double mutant *pf1-1 adh1* (33), which lacks the pyruvate formate-lyase and the alcohol dehydrogenase involved in fermentation pathways; the ATP synthase mutant *Fud50.OR+* (34), the $\Delta rbcL$ 1-7.5 mutant, which lacks the large subunit of Rubisco (35); the plastocyanin mutant *ac208* (36), the so-called *pewy* mutant, which accumulates the *b_f* complex but is impaired in its quinol oxidation site (37); the $\Delta petA$ mutant, which lacks *b_f* complex (38); the *dum22* mutant lacks both the mitochondrial complex I and *bc₁* complexes (39), and the *HydEF* (40) and *HydG* (41) mutants that lack assembly factors required for hydrogenase maturation. Cells were grown to mid-log phase (3–5 10^6 cells per ml) in Tris/acetate/phosphate medium (42) at 25 °C at 50 $\mu\text{mol photons m}^{-2} \text{s}^{-1}$.

Spectrophotometric Measurements—Cells were spun down at $2500 \times g$ for 5 min at 20 °C, and the pellet was resuspended in 20 mM HEPES, pH 7.2, 10% Ficoll to reach a final cell concentration of $\sim 6 \cdot 10^6$ cells per ml. The cell suspension was then vigorously stirred in a 50-ml Erlenmeyer flask for 30 min in the dark at 340 rpm. Absorption changes were measured as described previously (26) with a JTS-10 (Bio-Logic, Grenoble, France). The detecting and continuous lights were provided by LEDs and the saturating flash by a dye laser (640 nm) pumped by a second harmonic of an Nd:Yag laser (Minilite II, Continuum). The detection wavelength was selected using interferential filters, 520 nm, 10 nm full width at half-maximum; 546, 705,

and 730 nm, 6 nm full width at half-maximum. Blue (BG-39, Schott) and red (RG 695) filters were used to cut off the excitation light. To assess the absorption changes associated with the redox changes of P_{700} , the absorption changes measured at 730 nm were subtracted to correct for unspecific contribution at 705 nm. Similarly, the electrochromic shift signal, which yields an absorption change that is linearly related to the transmembrane electric field (43, 44), was estimated after subtraction of the absorption changes measured at 546 nm to those measured at 520 nm. Strict anoxia was reached by addition of glucose oxidase (type II, *Aspergillus niger*, 2 mg ml⁻¹) and glucose (20 mM). DCMU (10 μM) was added just before measurement to inhibit PSII.

Assessment of Cyclic Electron Flow—Cyclic electron flow was estimated as described previously (26), in the presence of 10 μM DCMU to inhibit PSII activity. Under continuous illumination, at steady state, $k_{\text{ox}} [P_{700}^{\text{red}}] = k_{\text{red}} [P_{700}^{\text{ox}}]$, where k_{ox} is the oxidation rate of P_{700} , which is a convolution of the light intensity and the PSI absorption cross-section. It was assessed by measuring the initial slope of the rising electrochromic shift signal upon the onset of continuous illumination, as described previously (26). k_{red} is the reduction rate of P_{700}^{ox} . The electron flux sustained under these conditions is simply the product between k_{ox} and P_{700}^{red} .

P_{700} Oxidation Kinetics—To follow the spontaneous reoxidation of the stromal electron acceptor pool (see text for details), the cells were kept in the dark in strict anoxic conditions. After 5, 20, and 40 min, the extent of photo-oxidizable P_{700} was assessed by applying a 40-ms pulse of saturating light after 10 s of continuous illumination. We checked that this yielded the maximum extent by shortening or increasing the duration of the pulse. To follow the alleviation of the PSI acceptor side limitation (32) induced by continuous illumination, the cells were placed in anoxia for 5 min. Then PSI oxidation yield was assessed by a pulse of saturating actinic light superimposed to the continuous light used to abrogate the PSI acceptor side limitation. The absorption changes associated with the full oxidation of P_{700} was assessed in the presence of 10 μM DCMU in oxic conditions.

Hydrogen Evolution—Hydrogen evolution was measured using an oxygen-sensitive Clark-type oxygen electrode (Oxygraph, Hansatech Instruments) modified to only detect hydrogen (Oxy-Ecu, Hansatech Instruments). The entire setup was placed in a plastic tent under anoxic atmosphere (N₂) to avoid contamination of anaerobic samples by oxygen while filling the measuring cell of the oxygraph. As for the spectrophotometric experiments, strict anoxia was reached by addition of glucose oxidase (type II, *A. niger*, 2 mg ml⁻¹) and glucose (20 mM). DCMU (10 μM) was added just before measurement to inhibit PSII.

RESULTS

As mentioned above, we reported in Ref. 26 that upon the onset of anoxia the light-induced oxidation of P_{700} is strongly impeded (31). We interpreted this limitation as resulting from the high proportion of PSI electron acceptors being in their reduced state prior to illumination, which would induce fast charge recombination and thus compete with productive elec-

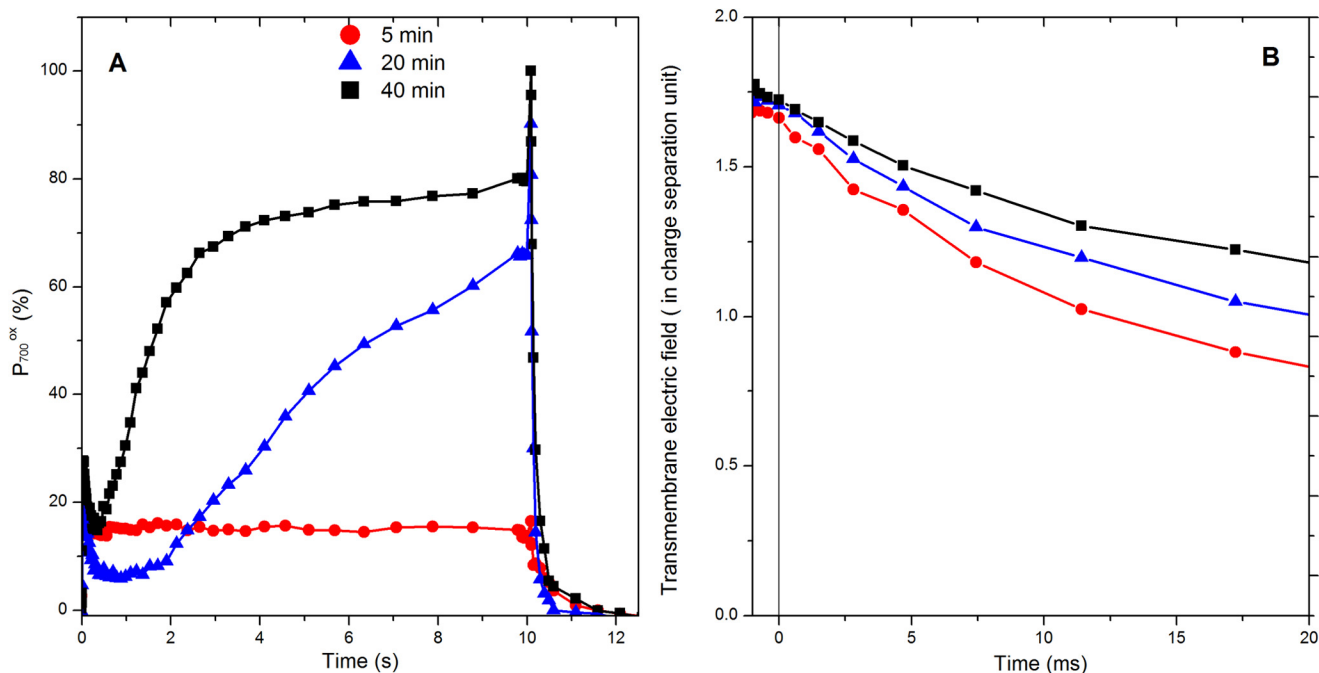


FIGURE 1. Comparison of the absorption changes associated with the redox changes of P_{700} (A) and with the buildup of the transmembrane electric field (B) after increasing incubation time in anoxic conditions. A shows the light-induced absorption changes associated with P_{700} redox changes after 5 min (red), 20 min (blue), and 40 min (black) of incubation in anoxia. The cells were illuminated ($115 \mu\text{E}\cdot\text{m}^{-2}\cdot\text{s}^{-1}$) for 10 s, and the maximum amount of photo-oxidizable P_{700} was assessed by superimposing a 40-ms-long saturating pulse. Afterward, the reduction of P_{700} was followed in the dark. B shows the steady state level of the transmembrane electric field reached upon 10 s of illumination of cells incubated for 5 min (red), 20 min (blue), and 40 min (black) in anoxia, followed by its decay after the light has been switched off. The ordinate axis was calibrated in a charge separation unit using the electrochromic shift signal obtained after a single turnover flash. The slope of the decay taking place at the end of the 10 s of illumination provides an estimate of the rate at which the transmembrane electric field is produced, i.e. CEF in this case, and B shows they were similar ($\sim 30 \text{e}^{-}\cdot\text{s}^{-1}$ per PSI) in the three cases. In both A and B the kinetics are the average of three independent experiments, and the variation was below $\pm 10\%$.

tron transfer between PSI and the electron donors/acceptors upstream/downstream in the chain. However, a fraction of PSI must remain that still performs productive electron transfer because, in anoxic and inhibited PSII conditions, illumination of *Chlamydomonas* cells promotes the establishment of a transmembrane electric field (29). This is further illustrated in Fig. 1, which compares the light-induced redox changes of P_{700} and transmembrane electric field.

As reported previously (26), after ~ 40 min in the dark and anoxia,⁷ the fraction of oxidizable P_{700} , estimated by the signal after being induced by the saturating light pulse (32), reached 100% thus showing that the acceptor side limitation is spontaneously alleviated during this incubation. In turn, the light-induced transmembrane electric field reached after 10 s of illumination hardly changed with the duration of incubation in anoxia. The rate of its decay, observed when switching off the light and using as a measure of its generation by productive electron flow (45), was close to $50 \text{e}^{-}\cdot\text{s}^{-1}$ per PSI after ~ 5 min of anoxia in the dark and progressively decreased to reach $\sim 30 \text{e}^{-}\cdot\text{s}^{-1}$ per PSI after a prolonged incubation, although it

would be null in a mutant impaired in the photosynthetic electron transfer, e.g. lacking the b_6f complex (46). This suggests that the fraction of PSI engaged in productive turnovers rather than charge recombination, assessed by the superimposition of a saturating pulse to the continuous illumination, is seriously under-estimated. As already pointed out in Ref. 47, this is likely because the pulse induces multiple turnovers and may thus contribute to the building up of the charge recombining state(s), in particular when the fraction of P_{700} that remains to be oxidized by the multiple turnover pulse is large. To circumvent this methodological limitation, we resorted to single turnover flashes and assessed the fraction of photo-oxidizable PSI by the amplitude of the electrochromic absorption changes (520–546 nm) 140 μs after a saturating laser flash. When PSII is inhibited, this signal is proportional to the amount of reduced P_{700} prior to the flash. Fig. 2 shows the relative amplitude of this signal (normalized to the maximum associated with PSI charge separation) plotted against the fraction of P_{700} remaining reduced under illumination.

In such a plot, one would expect the data to stand on the diagonal because the two methods are meant to probe the same parameter. Clearly, this was not the case after 5 min of anoxia, where the assessment of the fraction of reduced P_{700} in the light was systematically larger than when assessed by the electrochromic shift. Notably, the deviation was observed at all light intensities tested here. The deviation decreased as the cells were incubated for longer times in the dark and anoxia, and the data fell on the diagonal after 40 min of incubation indicating a

⁷We note here that the duration of the incubation in the dark and anoxia required to reach the metabolic status corresponding to those described in the text and the figures should be taken as indicative and may vary between batches. The data shown in Fig. 1, A and B, are thus meant to illustrate the spontaneous evolution in the dark and anoxia and the time window during which it takes place rather than its accurate time course. Hereafter, 5, 20, and 40 min should thus be understood as the time typically required to reach the blocked, partially blocked, and deblocked states characterized by the data shown in Fig. 1, A and B.

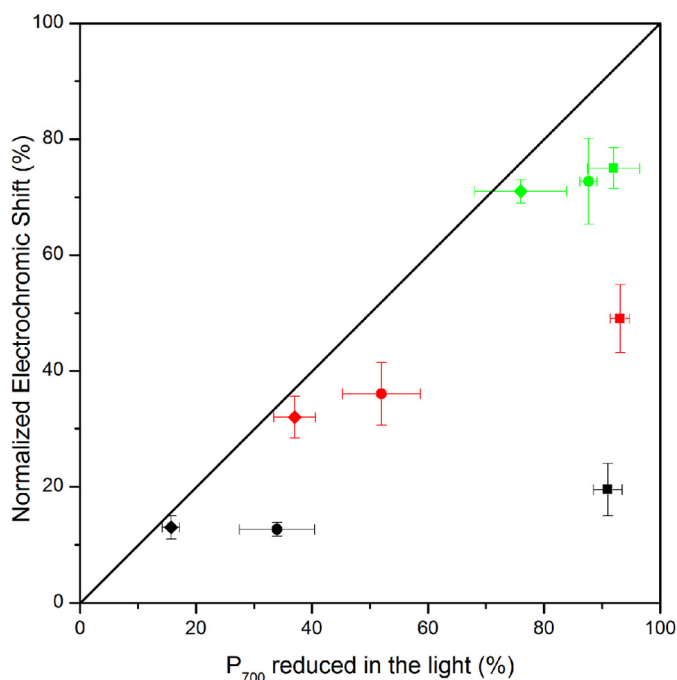


FIGURE 2. Comparison of two different methods aimed at assessing the fraction of P_{700} involved in electron flow. The x axis is the fraction of P_{700} remaining reduced under illumination assessed as the ratio between the steady state light-induced absorption change and the maximum one measured under aerobic conditions. The squares, circles, and diamonds, respectively, show the data obtained after 5, 20, and 40 min of anoxia at different illumination intensities ($20 \mu\text{E}\cdot\text{m}^{-2}\cdot\text{s}^{-1}$, green; $55 \mu\text{E}\cdot\text{m}^{-2}\cdot\text{s}^{-1}$, red; and $115 \mu\text{E}\cdot\text{m}^{-2}\cdot\text{s}^{-1}$, black). The y axis is the relative amplitude of the electrochromic shift measured 140 μs after a saturating laser flash normalized to its maximum amplitude obtained in oxic conditions. The kinetics are the average of three independent experiments.

satisfying agreement between the two methods. The noticeable difference between the fraction of photo-oxidizable P_{700} and the fraction that gives rise to a stable charge separation upon a single turnover flash provides additional support to the earlier proposal that a large fraction of PSI undergoes an acceptor side limitation. Importantly, and consistent with our previous analysis, after 40 min of anoxia, in darkness, the acceptor side limitation was alleviated as evidenced by the satisfying agreement between the fraction of photo-oxidizable PSI and that engaged in stable charge separation upon a single turnover flash (Fig. 2). At this stage, we may thus conclude that during the early times of anoxia, a major fraction of PSI undergoes a severe acceptor side limitation. Yet, this fraction is overestimated by the saturating light pulse method because the pulse induces multiple turnovers and thereby contributes to promoting charge recombination in a fraction of PSI which, prior to the pulse, is otherwise involved in productive electron flow.

Under steady state illumination conditions, the fraction of P_{700} being reduced is shown in Equation 1.

$$\frac{k_{\text{red}}}{k_{\text{red}} + k_{\text{ox}}} \quad (\text{Eq. 1})$$

Thus, to efficiently counteract the light-induced oxidation of P_{700} , the reduction rate must be significantly larger than the oxidation rate. In this framework, the observation that, after 5 min of anoxia in darkness (Fig. 2, squares), the steady state fraction of reduced of P_{700} did not decrease with increasing

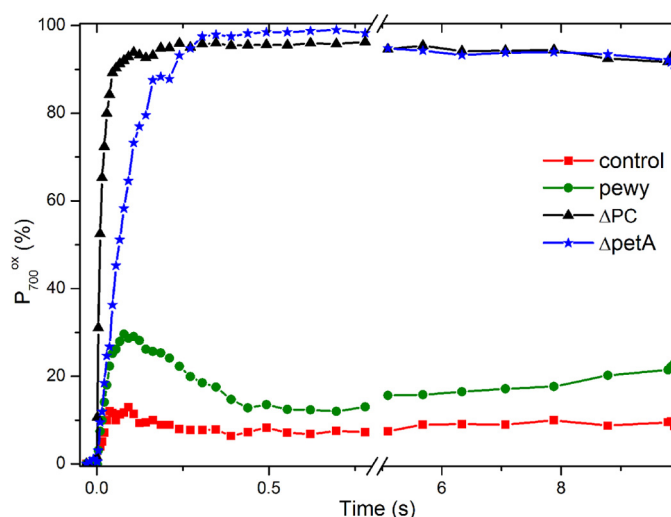


FIGURE 3. PSI acceptor side limitation in anoxia in various *C. reinhardtii* mutants impaired upstream of photosystem I. The kinetics of P_{700} were measured after 5 min of anoxia in the control (red square), the *pewy* mutant (green circle), ΔpetE (black triangle), and ΔpetA (blue stars). The light intensity was $115 \mu\text{E}\cdot\text{m}^{-2}\cdot\text{s}^{-1}$. The kinetics are the average of three independent experiments and the variation was below $\pm 10\%$.

light intensity (k_{ox}) suggests that the reduction rate, k_{red} , also increases with light intensity. This is diagnostic of charge recombination, the rate of which depends on the radical pair involved. We estimated in Ref. 26 that with a light intensity of $135 \mu\text{E}\cdot\text{m}^{-2}\cdot\text{s}^{-1}$, the PSI photochemical rate is $150 \text{e}^{-}\cdot\text{s}^{-1}$. Thus, 84% of P_{700} reduced at steady state (Fig. 1A) translates in a reduction rate faster than $\sim 800 \text{e}^{-}\cdot\text{s}^{-1}$ per PSI. Such a range is faster than the decay of the $P_{700}^{+}F_{A/B}^{-}$ state (48, 49), implying that the charge recombination process involves either the $P_{700}^{+}F_{X}^{-}$ radical pair or a faster decaying one such as $P_{700}^{+}A_{1}^{-}$ or even $P_{700}^{+}A_{0}^{-}$ (see Ref. 29 and see Ref. 49 and references therein). Yet, after 5 min of darkness and anoxia, a single turnover flash generates a radical pair that is much longer lived than any of these states as evidenced by the long lived transmembrane electric field observed under such conditions (50–52). Thus, these fast charged recombining states accumulate during the continuous illumination because of the congestion of the electron flow downstream.

This raises the question of the redox state of the PSI electron acceptors prior to the illumination. To address this, we assessed the extent of the acceptor side limitation in various *C. reinhardtii* mutants impaired upstream of PSI. We reasoned that if indeed the charge recombining state is formed after several photochemical turnovers, which progressively lead to the reduction of the pool of electron acceptors, the extent of the light-induced promotion of the fast charge-recombining state should depend on the size of the pool of electron donors. Consistent with this, we did not observe any acceptor side limitation in mutants lacking either the plastocyanin or the b_6f complex (Fig. 3).

Thus, in the absence of the b_6f complex, the number of reducing equivalents available upstream of PSI is insufficient to fill the pool of downstream electron acceptors and to promote the formation of the fast recombining state. Because the number of turnovers undergone by P_{700} before it is fully oxidized is proportional to the area above the oxidation curve, the pool of the

Metabolic Remodeling on a Shift to Anoxia in *C. reinhardtii*

electron donor can be assessed, relative to the PSI content, by the ratio between the area above the P_{700} oxidation kinetics obtained in the b_6f -lacking strain with that obtained with the plastocyanin-lacking strain (which, after normalization of the maximal signal associated with P_{700} oxidation between the different strains, can be normalized to 1 because, in this case, a single photochemical act per PSI leads to the oxidation of P_{700}). We thereby estimate the pool in the b_6f to 2.7, which is in good agreement with the previous estimates of the plastocyanin to PSI stoichiometry (53). Thus, in the dark after 5 min of anoxia, the pool of PSI electron acceptor oxidized in the dark per PSI exceeds 3.7 (2.7 plastocyanin + P_{700}). To further characterize the overall redox state of the pool of PSI electron acceptors, we relied on the so-called *pewy* mutant in which b_6f accumulates to wild type-like levels but is inactive in quinol:plastocyanin oxidoreductase activity (37). In this mutant, we estimated, in oxic conditions, the pool of electron donor to 7–8, which is only slightly above the expected 5.7 stoichiometry (1 P_{700} + 2.7 plastocyanin + the Rieske FeS cluster and cytochrome *f*). After 5 min of anoxia, in darkness, the P_{700} oxidation state reached after illumination was close to but not exactly equal to 100%, suggesting that, fortuitously but fortunately, the number of available oxidized electron acceptors is commensurate to the pool of reducing equivalents available upstream of PSI. Thus, taking into account the fact that the F_A and F_B iron-sulfur cluster must be reduced before the $P_{700}^+F_X^-$ state accumulates, we estimate that, per PSI, only ~4–5 soluble electron acceptors (ferredoxin, FNR, and $NADP^+$) are in the oxidized state, in the dark, after 5 min of anoxia. With midpoint potentials of –420 mV (54), –345 mV (55), and –320 mV and stoichiometries relative to PSI of 4, 2, and 5 for ferredoxin, FNR, and $NADP^+$, respectively (56–58 and references therein), this translates, assuming that equilibrium is achieved in the dark, to an ambient redox potential of approximately –370 mV after a few minutes of anoxia. This is only mildly more reducing than the redox poise –320 mV reported in the plastid of epidermal cells in *A. thaliana* (59) and hardly less than the estimate made previously (29) of the steady redox poise in the stroma of *C. reinhardtii* in the light in anoxia.

One of the outcomes of the results described previously (26) is that, as further illustrated in Fig. 1A, the acceptor side limitation is progressively relieved with the incubation of the cells in anoxic conditions. In the present framework, this would result from the progressive reoxidation, in the dark, of the PSI electron acceptors. Incidentally, we note here that this spontaneous relief of the acceptor side limitation did not take place when the cells were incubated in the presence of hydroxylamine in addition to DCMU. This inhibitory effect of hydroxylamine remains to be understood, but its use was systematically avoided in our previous and present studies. A possible way to test the above statement that the acceptor side limitation is relieved because of progressive reoxidation of the PSI electron acceptors is to attempt to promote or hamper this reoxidation and assess the consequences on the relative fraction of charge recombining PSI centers. A straightforward way to promote the reoxidation is to activate the Bassham-Benson-Calvin cycle by supplying it with ATP. According to the above estimate of the ambient redox potential in the cells in anoxia, the $NADP^+$ pool

should be almost fully reduced in the dark so that the mere supply of ATP should suffice to promote CO_2 fixation and thus NADPH consumption.

Because we have shown above that, even when the acceptor side limitation is the more pronounced, a protonmotive force builds up upon illumination, we simply relied on light to modulate the intracellular ATP content. Cells were placed in anoxia and, after 5 min of incubation in the dark, they were submitted to illumination. We followed the steady state level and fraction of photo-oxidizable P_{700} during the time course of the illumination. As shown in Fig. 4, the fraction of photo-oxidizable P_{700} reached 100% after only 90 s of illumination, *i.e.* much earlier than when keeping the cells in the dark where the spontaneous alleviation took place in the tens of minute time range (see Figs. 1A and 4A). Yet, during this time lapse many PSI turnovers take place because the CEF rate is in the 30–60 $e^- \cdot s^{-1}$ per PSI implying that the limiting step in the process is not an individual electron transfer step in the cyclic process. As expected, illumination was inefficient in promoting the relief of the acceptor side limitation when repeating the experiment with the *Fud50* mutant that lacks the CF_0F_1 -ATP synthase (34, 60), demonstrating that the light-induced reoxidation of the electron acceptors is ATP-dependent. To further characterize the involvement of the CO_2 fixation pathway, we conducted a similar experiment with a Rubisco-lacking mutant (35).

At variance with the clear-cut *Fud50* case, illumination did progressively palliate the acceptor side limitation with a similar time course than in the control strain but to a smaller extent. In the present framework, this suggests that, despite the absence of Rubisco, the reoxidation of the pool of electron acceptors does occur but remains partial so that a fraction of PSI still undergoes charge recombination. Even though it may seem otherwise at first sight, this result is not contradictory to our hypothesis that the reoxidation of the PSI electron acceptors results from the onset of the CO_2 -reducing pathway promoted by the light-induced increase in ATP. Indeed, there are two ATP-requiring enzymatic steps in the Bassham-Benson-Calvin cycle as follows: 1) the phosphorylation of 3-phosphoglycerate, which provides the substrate of the NADPH-consuming production of glyceraldehyde 3-phosphate, and 2) the phosphorylation of ribulose-5-phosphate to ribulose-1,5-bisphosphate, the substrate of Rubisco (61). The advancement of either step may allow NADPH oxidation, respectively, through the production of the substrate or the consumption of the product of the NADPH-consuming step. Thus, provided the pool of 3-phosphoglycerate is sufficiently large, ATP production may promote NADPH consumption even in the absence of a completely active CO_2 -reducing pathway. To assess this hypothesis, we used glycolaldehyde (62) or iodoacetamide (20 mM) to inhibit each one of these two ATP-dependent reactions. Whereas iodoacetamide induced severe side effects, such as strong fluorescence quenching, we found glycolaldehyde to be reasonably specific in agreement with previous studies (62, 63). As shown in Fig. 4B, addition of glycolaldehyde hampered the light-induced relief of the PSI acceptor side limitation, yet without canceling it completely.

The protocol used to follow the progressive alleviation of the acceptor side limitation upon illumination allows determining

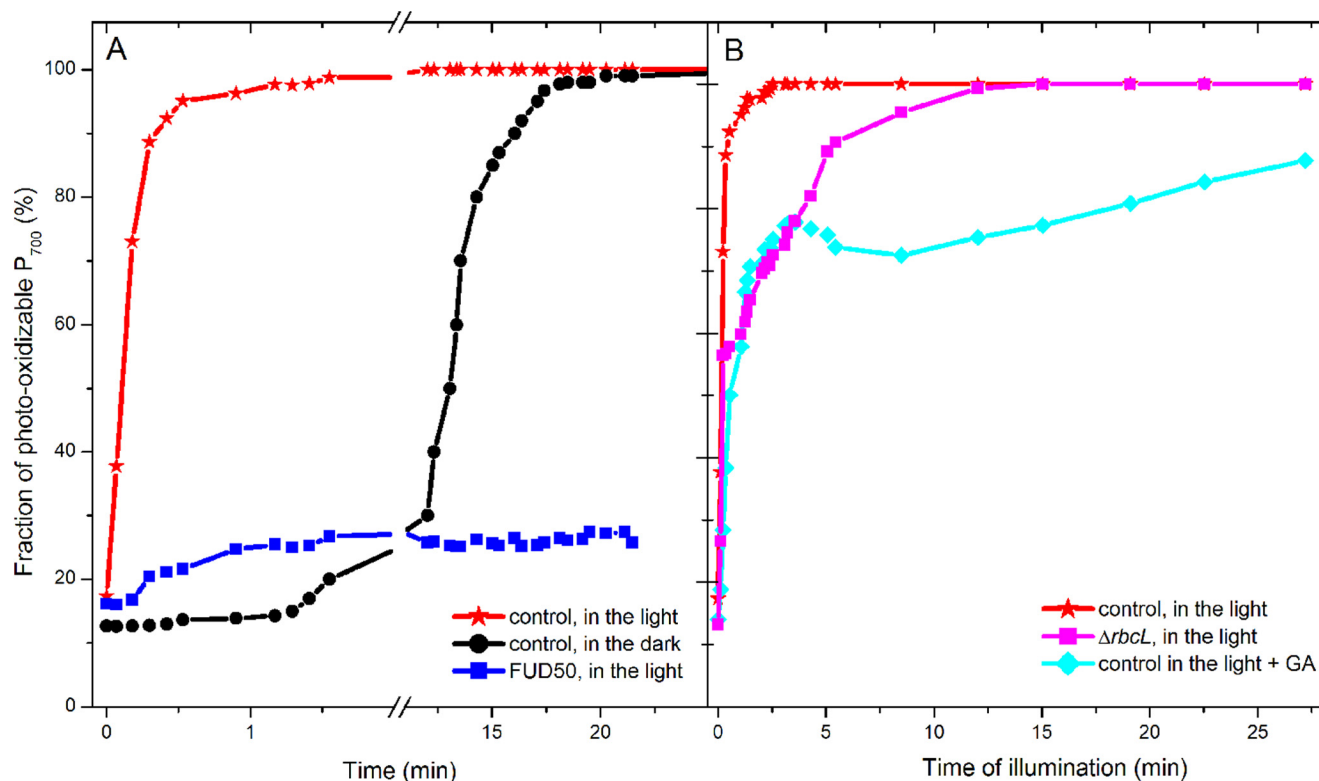


FIGURE 4. Evolution of the PSI acceptor side limitation as a function of the time in anoxia or of illumination. The light intensity was $115 \mu\text{E}\cdot\text{m}^{-2}\cdot\text{s}^{-1}$ intensity. *A*, after 5 min of anoxia in the dark, continuous light was applied, and the resulting alleviation of the PSI acceptor side limitation was probed at discrete times by assessing the extent of P₇₀₀ photo-oxidation upon a saturating pulse. *Black* indicates control strain in the dark; *red* indicates control strain in the light; and *blue* indicates *Fud50* strain in light. *B*, as in *A* when the Bassham-Benson-Calvin cycle is inhibited, due to either the absence of Rubisco, $\Delta rbcL$ (in *magenta*), or to addition of glyceraldehyde inhibitor ($20 \mu\text{M}$ (62)). Three independent experiments were averaged, and the variation was below $\pm 10\%$.

the progressive increase in the photochemical yield of PSI, measured as the difference between the oxidation state of P₇₀₀⁺ in steady state conditions and that obtained after a saturating pulse, over the signal corresponding to the full oxidation of P₇₀₀. As discussed previously (26), multiplying this yield by the photochemical rate of PSI provides the flux sustained by PSI. The time course of this flux is shown in Fig. 5 and compared with the value obtained after the spontaneous full recovery of PSI activity in the dark. We found that the apparent CEF rate increased during the 1st min of illumination. It then reached a maximum after 1–2 min of illumination and then decreased to an asymptotic value similar to the one reached after a prolonged incubation in the dark. As shown above, the first tens of seconds of illumination correspond to a time period during which the system undergoes the acceptor side limitation, so that, as discussed above, the CEF low rate found reflects the low PSI photochemical yield.

Following this tens of minutes, we found that CEF rates transiently exceeded the asymptotic level reached after the progressive reoxidation of the PSI acceptor pool in the dark. This is consistent with the proposals that CEF is enhanced when the PSI electron acceptors are reduced and that their reduction state is likely to be the limiting factor (26, 28, 29). The intensity of the flux then decreased to reach a steady state value similar to the one observed after the spontaneous reoxidation of the PSI acceptor pool. Such transient large CEF fluxes are commensurate with values found in plants under conditions aimed at promoting CEF *versus* LEF (64). As discussed previously (65, 66),

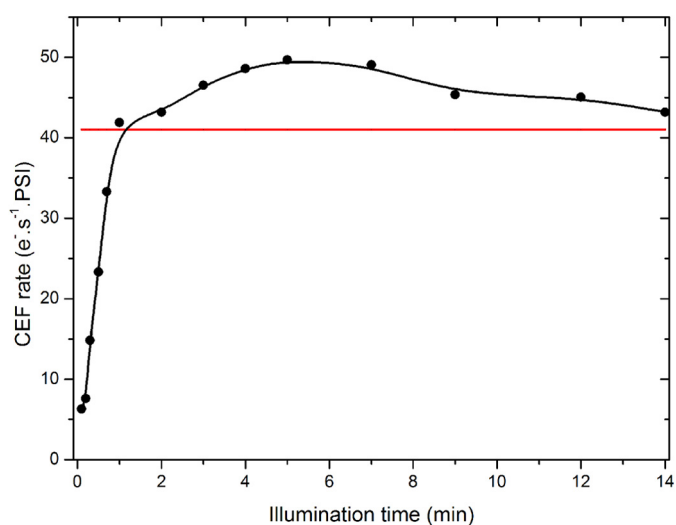


FIGURE 5. CEF as a function of the duration of illumination in anoxia. The *data points* show the value of CEF measured as in Ref. 26 at discrete times after the onset of illumination in anoxic control cells. The *red line* shows the value of CEF reached after the spontaneous alleviation of the PSI acceptor limitation after 40 min of incubation in the dark. Three independent experiments were averaged, and the variation was below $\pm 10\%$.

because of the inhibition of PSII, illumination is indeed expected to promote the oxidation of the plastoquinone pool and further reduce, with respect to its dark-adapted case, the electron acceptor pools. This is expected to yield optimal conditions because the pools of reactants and products of the step

TABLE 1

Characterization of the various strains studied here with respect to the alleviation of the PSI acceptor side limitation

Strains	PSI acceptor side limitation after 5 min of anoxia	PSI acceptor side limitation after 40 min of anoxia in the dark	Light-induced alleviation of the acceptor side limitation
T222+	Yes	No	Yes
<i>Hyd EF</i>	Yes	Yes	~85%
<i>Hyd G</i>	Yes	Yes	Yes
<i>pfl1,adh</i>	Yes	No	Yes
<i>FUD 50</i>	Yes	~20%	No
<i>Δrbcl 1</i>	Yes	~20%	~85%
T222+ (+ hydroxylamine)	Yes	Yes	~95%

considered as being limiting are maximal and minimal, respectively (29). The progressive decrease in the CEF rate observed upon a prolonged illumination would then simply reflect the progressive reoxidation of the electron acceptor pool because of the ATP-dependent pathways. Importantly, as already pointed out in Refs. 29, 67, the observation that after a few minutes of illumination CEF reaches a steady state value implies that the “leak” of reducing power resulting from the CO₂-reducing pathway, the implication of which has been discussed above, is compensated for by a constant influx of reducing power, which likely stems from starch and glucose catabolism (68).

Now that we have demonstrated that the reoxidation of the pool of electron acceptors is sufficient to alleviate the unproductive buildup of charge-recombining PSI, we may reason that, similarly, the spontaneous consumption of reducing power is responsible for the alleviation of the acceptor side limitation after a prolonged incubation of anoxia in the dark. Several metabolic pathways can be readily identified as likely candidate(s), among which the fermentation pathway and the hydrogen-producing pathway are prominent (6–10). To characterize their possible involvement, we studied the occurrence of the spontaneous relief of the acceptor side limitation in *Chlamydomonas* mutants specifically deficient in key enzymes in these two pathways.

We first studied the double mutant *pfl1,adh* (33), deficient in two enzymes of the predominant fermentative pathways, pyruvate formate-lyase and alcohol dehydrogenase. With regard to the spontaneous reoxidation in the dark of PSI electron acceptor pool, the mutant hardly differed from the control strain (in this case *CC125*). Yet, this negative results does not rule out the contribution of fermentative pathways because Catalanotti *et al.* (33) have shown that the induction of an alternative fermentation pathway compensates for the absence of PFL1 and alcohol dehydrogenase activity.

The transition from aerobic to anaerobic conditions is known to promote a massive reorganization of the metabolism of *C. reinhardtii* as evidenced by the numerous genes regulated at the transcriptional level (6–9). We thus asked whether the transition we observed in the dark requires the induction of a specific nuclear gene and protein neosynthesis. We thus compared the time course of the transition in the presence and absence of cycloheximide (15 μg·ml⁻¹). Because it has been reported that microanaerobic conditions can be promoted simply by spinning down the cells to collect them (4), the protein neosynthesis inhibitor was added prior to centrifugation and to the resuspension buffer. The cells were then vigorously shaken under dim light for 60 min. This led to a significant slowing down of the spontaneous relief of the acceptor side limitation in

the dark (data not shown), thus suggesting that the process involves *de novo* protein synthesis. This result is in line with the recent finding that the acceptor side limitation undergone by PSI persists for a longer time in the absence of hydrogenase than in the control strain (31). Indeed, this activation is notoriously regulated at the transcription level upon anoxia (69). Thus, as regards the presence or absence of this activity, one would expect the inhibition of protein neosynthesis to mimic a knock-out mutant.

We thus checked whether the hydrogenase activity is indeed involved in the control of the redox poise in the dark and compared the time course of this transition in the *hydEF* (40) and *hydG* (41) mutants both described as being deficient in hydrogenase activity because of the lack of proper assembly of the catalytic center (70). We consistently found that, in these two mutants, the acceptor side limitation remained after a prolonged incubation in the dark (see Table 1) in agreement with Ghysels *et al.* (31).

This stresses out the consumption of reducing power by the hydrogen production pathway as being the main process responsible for the alleviation of the PSI acceptor side limitation. According to the above estimate, the reducing pressure in anoxia is such that the ferredoxin pool is partly reduced in the dark. Hydrogen production may thus spontaneously take place under these conditions by the uphill and sequential electron transfer from NADPH to ferredoxin and then hydrogenase or the combined involvement of the pyruvate ferredoxin oxidoreductase and the hydrogenase (33). Alternatively, the progressive buildup of the hydrogenase activity because of the increased transcription of its gene may open up an electron sink so that the short illumination in the presence of DCMU would effectively contribute to producing oxidizing equivalent. In any event, as shown in Fig. 6, the direct measure of hydrogen production confirmed that, in agreement with previous studies (11, 31, 71), the hydrogenase is expressed.

In the presence of DCMU, *i.e.* similar conditions as when measuring P₇₀₀ redox changes, the light-induced production rates of hydrogen at the very early stage after the onset of anoxia were 28 and 75 nmol of H₂·(min·mg of Chl)⁻¹ after 5 and 40 min of anoxia, respectively. The latter rate is ~30–40-fold slower than the light-driven oxygen evolution rate typically found in *C. reinhardtii* (69), so that it can be estimated to ~3 e⁻·s⁻¹ per PSI. When measured in the dark, the hydrogen production rate was below detection after 5 min of anoxia and 10 nmol of H₂·(min·mg of Chl)⁻¹ after 40 min. When expressed in e⁻·s⁻¹ per PSI units, such a rate corresponds to ~0.4.

The present results show that the onset of anoxia promotes, in the dark, the reduction of a significant fraction of the PSI

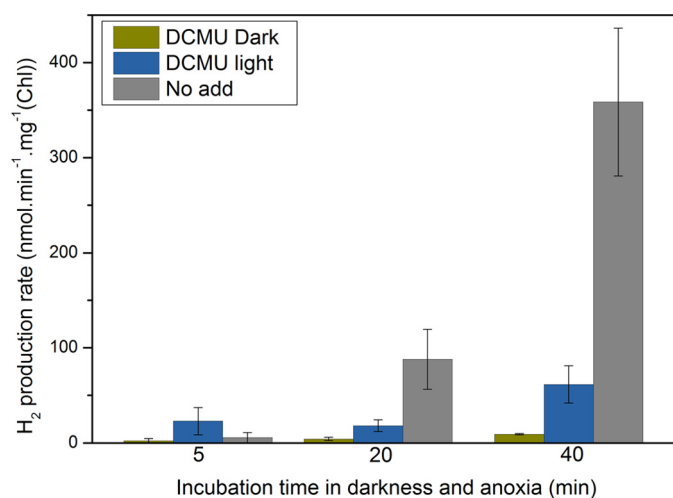


FIGURE 6. **Hydrogen production rates as a function of incubation time in anoxia.** After the indicated incubation time, the hydrogen production rate was determined as the slope of the increase in hydrogen amount as a function of time. When the light-induced hydrogen production was measured, the light was applied for 1 min ($100 \mu\text{mol photons m}^{-2} \text{s}^{-1}$) in presence or absence of DCMU ($10 \mu\text{M}$). All measurements were performed at least in triplicate, and data are presented as means \pm S.D.

electron acceptors, likely by the mere shutdown of the oxidative pathways at work in oxic conditions, prominent among which are mitochondrial respiration and the PTOX pathway (15). In oxic conditions, the influx of reducing power resulting from chlororespiration has been estimated to be $2 e^{-} \cdot \text{s}^{-1}$ per PSI (67). To assess it in anoxic conditions, we followed the same procedure as in Ref. 67, *i.e.* we measured the half-time of reduction of P_{700}^{+} after its light-induced oxidation in the presence of methyl viologen (10 mM concentration) as an exogenous electron acceptor. This was performed with the *dum22* mutant, which has impaired mitochondrial respiration and should therefore constitutively mimic the redox situation of a wild-type strain with arrested mitochondrial respiration because of anoxia. According to this estimate, in anoxic conditions the light-independent influx would be similar as in oxic conditions, suggesting that, in actual fact, the arrest of the oxidizing activity of PTOX, rather than an increased influx of reducing power stemming from the metabolic exchange with the cytoplasm, is responsible for the increase in reducing redox pressure in the chloroplast.

DISCUSSION

We have shown here that the metabolic remodeling occurring upon anoxia in *C. reinhardtii* (see Ref. 72 for a recent proteomic and metabolomics survey) results in a transient reductive burst that promotes the almost complete reduction of the PSI electron acceptors in the dark. We estimate the size of the pool remaining oxidized to 7–8 oxidizing equivalents per PSI, which translates to an ambient redox potential of -370 mV . Yet, the over-reduction of the PSI electron acceptors turned out to be only transient. Indeed, we observed that the PSI electron acceptor limitation is spontaneously relieved in the dark. Based on the study of various mutants potentially affected in the pathways consuming these reductants, we identify the hydrogenase activity that builds up upon anoxia as the main pathway accounting for this alleviation. At this stage, it is interesting to

compare this activity to the influx of reducing equivalents promoted by glycolysis and all the catabolic pathways activated in anoxia. We estimated the latter to $\sim 2 e^{-} \cdot \text{s}^{-1}$ per PSI. With regard to the light-induced hydrogenase activity, the rate found after incubation for 40 min in anoxia and darkness is commensurate to, or slightly larger than, this influx, while it remains much lower after only 5 min. Thus, consistent with the present findings, several tens of minutes of progressive upscaling of the hydrogenase activity are necessary to let it outcompete the sluggish but significant influx and thereby allow, as soon as the light is switched on, the reoxidation of the PSI electron acceptors. At the onset of anoxia, the outflux of reducing power sustained by the hydrogenase activity that has just started to be expressed is still, according to the present estimates, 5-fold slower than the reducing influx, leaving the latter strong enough to promote the almost complete reduction of the pool of PSI electron acceptors, as estimated here.

The above analysis provides a consistent picture of the main electron fluxes occurring in the dark and highlights the role of the hydrogenase upon the onset of anoxia. Yet, illumination expectedly overturns the hierarchy. Indeed, we found that alleviation of the PSI acceptor side limitation is significantly faster under illumination, even though the PSII activity was blocked by DCMU thereby preventing the net photosynthetic production of reducing power and restraining the photosynthetic outcome to CEF and ATP synthesis. This is in line with the above framework because the light-driven synthesis of ATP is expected to activate all the ATP-dependent pathways that consume reducing power, prominent among which is the Bassham-Benson-Calvin cycle. The paramount implication of the light-induced ATP synthesis was demonstrated by the lack of light-induced relief of the PSI acceptor side limitation in the absence of a functional cF_0F_1 -ATP synthase. Importantly, the hydrogenase-lacking mutants were indistinguishable from the control strains with respect to this observation, thus showing that the light-induced electron consumption of reducing power hardly involves the hydrogenase when PSII is blocked. Consistently the hydrogen production pathway remains, upon the onset of anoxia, far below the light-induced electron flow and strictly dependent on the nonphotochemical reduction of the plastoquinone pool by Nda2.

Incidentally, the present observation allows one to rationalize the observation made by Bulté *et al.* (13) that, at variance with a control strain, cF_0F_1 -ATP synthase-lacking mutants remain locked in state 2 in anaerobic conditions even when illuminated in the presence of DCMU. Indeed, if, as shown here, a large majority of PSI remains doomed to undergo charge recombination, illumination inefficiently drains out the reducing pressure, and the plastoquinone pool remains reduced thereby locking these algae in state 2.

A careful assessment of the rate of cyclic electron flow upon the progressive light-induced alleviation of the PSI acceptor side limitation showed that it transiently reaches values up to $50 e^{-} \cdot \text{s}^{-1}$ per PSI and decreases until it reaches a plateau of $\sim 30\text{--}40 e^{-} \cdot \text{s}^{-1}$ per PSI. This evolution as a function of the light-induced change in the stromal redox poise prompted us to address the debated matter of the reliable determination of CEF (28, 29, 47, 66, 73). A survey of the literature shows that the

Metabolic Remodeling on a Shift to Anoxia in *C. reinhardtii*

reported rates for CEF are widely scattered, ranging from 10 to $20 \text{ e}^- \cdot \text{s}^{-1}$ per PSI in *Chlamydomonas* in oxic conditions (see Ref. 29 and references therein) to 40 to $60 \text{ e}^- \cdot \text{s}^{-1}$ per PSI in *Chlamydomonas* in anoxic conditions (see Ref. 29 and references therein), and up to $120\text{--}130 \text{ e}^- \cdot \text{s}^{-1}$ per PSI in spinach leaves (64, 74). Even though other physiological parameters, such as reactive oxygen species (75, 76) or ion transport (25, 77, 78), may contribute to the regulation of CEF, it is now widely agreed that the activation of cyclic is redox-controlled (28, 29, 47, 66, 73, 79). The scatter may thus simply reflect different physiological, redox, conditions. Alternatively, it may stem from the different approaches, methods, or tools used to assess this rate (29, 47, 73, 80). Walking in the steps of Bendall and Manasse (65), it has been emphasized recently that two boundary conditions exist, and between them CEF is expected to reach a maximum value. These two boundaries were defined as the two extreme cases where the steady state of both of the NADP^+ (NADPH) and quinol (quinone) pools would be fully oxidized (reduced), because, under such conditions, the concentration of either one of the two substrates of cyclic would be null (29, 81). We disagree with this presentation for the two following reasons. (i) This (over)simple description neglects the fact that CEF is a flux, the intensity of which is determined by the product between a concentration and a rate constant so that it may be significant even when the concentration of the substrate seems negligible.⁸ (ii) Under saturating conditions and in the presence of DCMU, the plastoquinone pool will effectively be oxidized and the electron donor pool reduced if, and only if, the kinetically limiting step in CEF is the reduction of the plastoquinone, an assumption that is kept implicit by the reasoning above and that remains, in any case, to be experimentally established. However, this presentation provides a useful framework by highlighting the fact that, at variance with a proper rate constant, a flux is, in essence, subjected to adjustments. This simple statement provides a straightforward explanation to the evolution of the CEF reported here as occurring upon the light-induced alleviation of the PSI acceptor side limitation. Indeed, we argued above that, starting from a situation where a majority of PSI undergoes fast charge recombination because of the entanglement of their downstream electron-accepting chain, illumination promotes the ATP-dependent oxidation of NADPH and thereby alleviates the acceptor side limitation. The progressive activation of this additional flux toward CO_2 reduction changes the steady redox state of the stromal electron carriers and diverts electrons from CEF thereby decreasing its efficiency. In this framework, the progressive decrease of CEF would thus simply reflect the transition from a situation where it is the only pathway at work to another one, established at steady state, where several competing pathways, such as CEF and LEF

⁸ To convince oneself, one may simply consider the steady states of the various redox players in linear electron flow under saturating illuminations; the plastoquinone pool is, almost, fully reduced, and plastocyanin is, almost, fully oxidized. Thus, the electron-accepting substrate of PSII is, at first sight, missing and so is the electron-donating substrate of PSI. Yet, the overall photosynthetic flow is maximal because the large photochemical rate compensates for the apparent lack of substrates. Notably, the point made here does not depend on the focus on any of the redox actors in the chain because, at steady state, the flux sustained by any of the individual steps in the chain is equal to the overall flux.

toward CO_2 or hydrogenase for example, would operate. Because the relative efficiency of these different pathways is regulated and depends on the metabolic status of the cell, it is unsurprising that variations are found among strains and even laboratories. As an illustration of this possible variability, we found different CEF rates under conditions where the PSI acceptor side limitation had been spontaneously relieved in the dark with the *T222* and *CC125* strains, both being supposedly comparable wild types.

REFERENCES

1. Steunou, A. S., Jensen, S. I., Brecht, E., Becraft, E. D., Bateson, M. M., Kilian, O., Bhaya, D., Ward, D. M., Peters, J. W., Grossman, A. R., and Kühl, M. (2008) Regulation of *nif* gene expression and the energetics of N_2 fixation over the diel cycle in a hot spring microbial mat. *ISME J.* **2**, 364–378
2. Hemschemeier, A., and Happe, T. (2005) The exceptional photofermentative hydrogen metabolism of the green alga *Chlamydomonas reinhardtii*. *Biochem. Soc. Trans.* **33**, 39–41
3. Mus, F., Dubini, A., Seibert, M., Posewitz, M. C., and Grossman, A. R. (2007) Anaerobic acclimation in *Chlamydomonas reinhardtii*: anoxic gene expression, hydrogenase induction, and metabolic pathways. *J. Biol. Chem.* **282**, 25475–25486
4. Dubini, A., Mus, F., Seibert, M., Grossman, A. R., and Posewitz, M. C. (2009) Flexibility in anaerobic metabolism as revealed in a mutant of *Chlamydomonas reinhardtii* lacking hydrogenase activity. *J. Biol. Chem.* **284**, 7201–7213
5. Yang, W., Catalanotti, C., D'Adamo, S., Wittkopp, T. M., Ingram-Smith, C. J., Mackinder, L., Miller, T. E., Heuberger, A. L., Peers, G., Smith, K. S., Jonikas, M. C., Grossman, A. R., and Posewitz, M. C. (2014) Alternative acetate production pathways in *Chlamydomonas reinhardtii* during dark anoxia and the dominant role of chloroplasts in fermentative acetate production. *Plant Cell* **26**, 4499–4518
6. Del Campo, J. A., Quinn, J. M., and Merchant, S. (2004) Evaluation of oxygen response involving differential gene expression in *Chlamydomonas reinhardtii*. *Methods Enzymol.* **381**, 604–617
7. Quinn, J. M., Eriksson, M., Moseley, J. L., and Merchant, S. (2002) Oxygen deficiency responsive gene expression in *Chlamydomonas reinhardtii* through a copper-sensing signal transduction pathway. *Plant Physiol.* **128**, 463–471
8. Hemschemeier, A., and Happe, T. (2011) Alternative photosynthetic electron transport pathways during anaerobiosis in the green alga *Chlamydomonas reinhardtii*. *Biochim Biophys Acta* **1807**, 919–926
9. Grossman, A. R., Croft, M., Gladyshev, V. N., Merchant, S. S., Posewitz, M. C., Prochnik, S., and Spalding, M. H. (2007) Novel metabolism in *Chlamydomonas* through the lens of genomics. *Curr. Opin. Plant Biol.* **10**, 190–198
10. Terashima, M., Specht, M., Naumann, B., and Hippler, M. (2010) Characterizing the anaerobic response of *Chlamydomonas reinhardtii* by quantitative proteomics. *Mol. Cell. Proteomics* **9**, 1514–1532
11. Hemschemeier, A., Melis, A., and Happe, T. (2009) Analytical approaches to photobiohydrogen production in unicellular green algae. *Photosynth. Res.* **102**, 523–540
12. Wollman, F.-A., and Bulté, L. (1989) *Towards an Understanding of the Physiological Role of State Transitions* (Hall, D. O., and Grassi, G., eds) pp. 198–207, Elsevier, Amsterdam
13. Bulté, L., Gans, P., Rebeille, F., and Wollman, F.-A. (1990) ATP control on state transitions *in vivo* in *Chlamydomonas reinhardtii*. *Biochim. Biophys. Acta* **1020**, 72–80
14. Jans, F., Mignolet, E., Houyoux, P. A., Cardol, P., Ghysels, B., Cuié, S., Cournac, L., Peltier, G., Remacle, C., and Franck, F. (2008) A type II NAD(P)H dehydrogenase mediates light-independent plastoquinone reduction in the chloroplast of *Chlamydomonas*. *Proc. Natl. Acad. Sci. U.S.A.* **105**, 20546–20551
15. Houille-Vernes, L., Rappaport, F., Wollman, F. A., Alric, J., and Johnson, X. (2011) Plastid terminal oxidase 2 (PTOX2) is the major oxidase involved in

- chlororespiration in *Chlamydomonas*. *Proc. Natl. Acad. Sci. U.S.A.* **108**, 20820–20825
16. Bonaventura, C., and Myers, J. (1969) Fluorescence and oxygen evolution from *Chlorella pyrenoidosa*. *Biochim. Biophys. Acta* **189**, 366–383
 17. Vallon, O., Bulte, L., Dainese, P., Olive, J., Bassi, R., and Wollman, F.-A. (1991) Lateral redistribution of cytochrome b6/f complexes along thylakoid membranes upon state transitions. *Proc. Natl. Acad. Sci. U.S.A.* **88**, 8262–8266
 18. Wollman, F. A., and Lemaire, C. (1988) Studies on kinase-controlled state transitions in Photosystem II and b6f mutants from *Chlamydomonas reinhardtii* which lack quinone-binding proteins. *Biochim. Biophys. Acta* **933**, 85–94
 19. Delosme, R., Olive, J., and Wollman, F. A. (1996) Changes in light energy-distribution upon state transitions—an *in vivo* photoacoustic study of the wild-type and photosynthesis mutants from *Chlamydomonas reinhardtii*. *Biochim. Biophys. Acta* **1273**, 150–158
 20. Iwai, M., Yokono, M., Inada, N., and Minagawa, J. (2010) Live-cell imaging of photosystem II antenna dissociation during state transitions. *Proc. Natl. Acad. Sci. U.S.A.* **107**, 2337–2342
 21. Nagy, G., Ünneper, R., Zsiros, O., Tokutsu, R., Takizawa, K., Porcar, L., Moyet, L., Petroutsos, D., Garab, G., Finazzi, G., and Minagawa, J. (2014) Chloroplast remodeling during state transitions in *Chlamydomonas reinhardtii* as revealed by noninvasive techniques *in vivo*. *Proc. Natl. Acad. Sci. U.S.A.* **111**, 5042–5047
 22. Ünlü, C., Drop, B., Croce, R., and van Amerongen, H. (2014) State transitions in *Chlamydomonas reinhardtii* strongly modulate the functional size of photosystem II but not of photosystem I. *Proc. Natl. Acad. Sci. U.S.A.* **111**, 3460–3465
 23. Finazzi, G., Furla, A., Barbagallo, R. P., and Forti, G. (1999) State transitions, cyclic and linear electron transport and photophosphorylation in *Chlamydomonas reinhardtii*. *Biochim. Biophys. Acta* **1413**, 117–129
 24. Finazzi, G., Rappaport, F., Furla, A., Fleischmann, M., Rochaix, J. D., Zito, F., and Forti, G. (2002) Involvement of state transitions in the switch between linear and cyclic electron flow in *Chlamydomonas reinhardtii*. *EMBO Rep.* **3**, 280–285
 25. Terashima, M., Petroutsos, D., Hüdig, M., Tolstygina, I., Trompelt, K., Gäbelein, P., Fufezan, C., Kudla, J., Weinl, S., Finazzi, G., and Hippler, M. (2012) Calcium-dependent regulation of cyclic photosynthetic electron transfer by a CAS, ANR1, and PGRL1 complex. *Proc. Natl. Acad. Sci. U.S.A.* **109**, 17717–17722
 26. Takahashi, H., Clowez, S., Wollman, F. A., Vallon, O., and Rappaport, F. (2013) Cyclic electron flow is redox-controlled but independent of state transition. *Nat. Commun.* **4**, 1954
 27. Wollman, F. A. (2001) State transitions reveal the dynamics and flexibility of the photosynthetic apparatus. *EMBO J.* **20**, 3623–3630
 28. Luckner, B., and Kramer, D. M. (2013) Regulation of cyclic electron flow in *Chlamydomonas reinhardtii* under fluctuating carbon availability. *Photosynth. Res.* **117**, 449–459
 29. Alric, J. (2014) Redox and ATP control of photosynthetic cyclic electron flow in *Chlamydomonas reinhardtii*: (II) involvement of the PGR5-PGRL1 pathway under anaerobic conditions. *Biochim. Biophys. Acta* **1837**, 825–834
 30. Iwai, M., Takizawa, K., Tokutsu, R., Okamuro, A., Takahashi, Y., and Minagawa, J. (2010) Isolation of the elusive supercomplex that drives cyclic electron flow in photosynthesis. *Nature* **464**, 1210–1213
 31. Ghysels, B., Godaux, D., Matagne, R. F., Cardol, P., and Franck, F. (2013) Function of the chloroplast hydrogenase in the microalga *Chlamydomonas*: the role of hydrogenase and state transitions during photosynthetic activation in anaerobiosis. *PLoS one* **8**, e64161
 32. Klughammer, C., and Schreiber, U. (1994) An improved method, using saturating light pulses, for the determination of photosystem I quantum yield via $P700^+$ -absorbance changes at 830 nm. *Planta* **192**, 261–268
 33. Catalanotti, C., Dubini, A., Subramanian, V., Yang, W., Magneschi, L., Mus, F., Seibert, M., Posewitz, M. C., and Grossman, A. R. (2012) Altered fermentative metabolism in *Chlamydomonas reinhardtii* mutants lacking pyruvate formate lyase and both pyruvate formate lyase and alcohol dehydrogenase. *Plant Cell* **24**, 692–707
 34. Lemaire, C., and Wollman, F. A. (1989) The chloroplast ATP synthase in *Chlamydomonas reinhardtii*. II. Biochemical studies on its biogenesis using mutants defective in photophosphorylation. *J. Biol. Chem.* **264**, 10235–10242
 35. Johnson, X., Wostrickoff, K., Finazzi, G., Kuras, R., Schwarz, C., Bujaldon, S., Nickelsen, J., Stern, D. B., Wollman, F. A., and Vallon, O. (2010) MRL1, a conserved pentatricopeptide repeat protein, is required for stabilization of rbcL mRNA in *Chlamydomonas* and *Arabidopsis*. *Plant Cell* **22**, 234–248
 36. Quinn, J., Li, H. H., Singer, J., Morimoto, B., Mets, L., Kindle, K., and Merchant, S. (1993) The plastocyanin-deficient phenotype of *Chlamydomonas reinhardtii* Ac-208 results from a frame-shift mutation in the nuclear gene encoding preapoplastocyanin. *J. Biol. Chem.* **268**, 7832–7841
 37. Zito, F., Finazzi, G., Delosme, R., Nitschke, W., Picot, D., and Wollman, F. A. (1999) The Qo site of cytochrome b6f complexes controls the activation of the LHCII kinase. *EMBO J.* **18**, 2961–2969
 38. Rimbault, B., Esposito, D., Drapier, D., Choquet, Y., Stern, D., and Wollman, F. A. (2000) Identification of the initiation codon for the atpB gene in *Chlamydomonas* chloroplasts excludes translation of a precursor form of the β subunit of the ATP synthase. *Mol. Gen. Genet.* **264**, 486–491
 39. Cardol, P., Gloire, G., Havaux, M., Remacle, C., Matagne, R., and Franck, F. (2003) Photosynthesis and state transitions in mitochondrial mutants of *Chlamydomonas reinhardtii* affected in respiration. *Plant Physiol.* **133**, 2010–2020
 40. Posewitz, M. C., King, P. W., Smolinski, S. L., Zhang, L., Seibert, M., and Ghirardi, M. L. (2004) Discovery of two novel radical S-adenosylmethionine proteins required for the assembly of an active [Fe] hydrogenase. *J. Biol. Chem.* **279**, 25711–25720
 41. Godaux, D., Emoncls-Alt, B., Berne, N., Ghysels, B., Alric, J., Remacle, C., and Cardol, P. (2013) A novel screening method for hydrogenase-deficient mutants in *Chlamydomonas reinhardtii* based on *in vivo* chlorophyll fluorescence and photosystem II quantum yield. *Int. J. Hydrog. Energy* **38**, 1826–1836
 42. Harris, E. H. (1989) *The Chlamydomonas Sourcebook*, pp. 25–64, Academic Press, San Diego
 43. Junge, W., and Witt, H. T. (1968) On the ion transport system of photosynthesis—investigations on a molecular level. *Z. Naturforsch. B.* **23**, 244–254
 44. Finazzi, G., and Rappaport, F. (1998) *In vivo* characterization of the electrochemical proton gradient generated in darkness in green algae and its kinetic effects on cytochrome b6f turnover. *Biochemistry* **37**, 9999–10005
 45. Sacksteder, C. A., and Kramer, D. M. (2000) Dark-interval relaxation kinetics (DIRK) of absorbance changes as a quantitative probe of steady-state electron transfer. *Photosynth. Res.* **66**, 145–158
 46. de Lacroix de Lavalette, A., Barucq, L., Alric, J., Rappaport, F., and Zito, F. (2009) Is the redox state of the ci heme of the cytochrome b6f complex dependent on the occupation and structure of the Qi site and vice versa? *J. Biol. Chem.* **284**, 20822–20829
 47. Baker, N. R., Harbinson, J., and Kramer, D. M. (2007) Determining the limitations and regulation of photosynthetic energy transduction in leaves. *Plant Cell Environ.* **30**, 1107–1125
 48. Hiyama, T., and Ke, B. (1971) A further study of P430: a possible primary electron acceptor of photosystem I. *Arch. Biochem. Biophys.* **147**, 99–108
 49. Brettel, K. (1997) Electron transfer and arrangement of the redox cofactors in photosystem I. *Biochim. Biophys. Acta* **1318**, 322–373
 50. Joliot, P., and Joliot, A. (1985) Slow electrogenic phase and intersystem electron transfer in algae. *Biochim. Biophys. Acta* **806**, 398–409
 51. Kramer, D. M., and Crofts, A. R. (1993) The concerted reduction of the high-potential and low-potential chains of the bf complex by plastoquinol. *Biochim. Biophys. Acta* **1183**, 72–84
 52. Finazzi, G., Büschlen, S., de Vitry, C., Rappaport, F., Joliot, P., and Wollman, F. A. (1997) Function-directed mutagenesis of the cytochrome b6f complex in *Chlamydomonas reinhardtii*: involvement of the cd loop of cytochrome b6 in quinol binding to the Q(o) site. *Biochemistry* **36**, 2867–2874
 53. Schöttler, M. A., Kirchoff, H., and Weis, E. (2004) The role of plastocyanin in the adjustment of the photosynthetic electron transport to the carbon metabolism in tobacco. *Plant Physiol.* **136**, 4265–4274

Metabolic Remodeling on a Shift to Anoxia in *C. reinhardtii*

54. Cammack, R., Rao, K. K., Barger, C. P., Hutson, K. G., Andrew, P. W., and Rogers, L. J. (1977) Midpoint redox potentials of plant and algal ferredoxins. *Biochem. J.* **168**, 205–209
55. Cassan, N., Lagoutte, B., and Sétif, P. (2005) Ferredoxin-NADP⁺ reductase. Kinetics of electron transfer, transient intermediates, and catalytic activities studied by flash-absorption spectroscopy with isolated photosystem I and ferredoxin. *J. Biol. Chem.* **280**, 25960–25972
56. Böhme, H. (1978) Quantitative determination of ferredoxin, ferredoxin-NADP⁺ reductase and plastocyanin in spinach chloroplasts. *Eur. J. Biochem.* **83**, 137–141
57. Moal, G., and Lagoutte, B. (2012) Photo-induced electron transfer from photosystem I to NADP(+): characterization and tentative simulation of the *in vivo* environment. *Biochim. Biophys. Acta* **1817**, 1635–1645
58. Antal, T. K., Kovalenko, I. B., Rubin, A. B., and Tyystjärvi, E. (2013) Photosynthesis-related quantities for education and modeling. *Photosynth. Res.* **117**, 1–30
59. Maughan, S. C., Pasternak, M., Cairns, N., Kiddle, G., Brach, T., Jarvis, R., Haas, F., Nieuwland, J., Lim, B., Müller, C., Salcedo-Sora, E., Kruse, C., Orsel, M., Hell, R., Miller, A. J., et al. (2010) Plant homologs of the *Plasmodium falciparum* chloroquine-resistance transporter, PfCRT, are required for glutathione homeostasis and stress responses. *Proc. Natl. Acad. Sci. U.S.A.* **107**, 2331–2336
60. Woessner, J. P., Masson, A., Harris, E. H., Bennoun, P., Gillham, N. W., and Boynton, J. E. (1984) Molecular and genetic analysis of the chloroplast ATPase of *Chlamydomonas*. *Plant Mol. Biol.* **3**, 177–190
61. Bassham, J. A., Benson, A. A., and Calvin, M. (1950) The path of carbon in photosynthesis. *J. Biol. Chem.* **185**, 781–787
62. Miller, A. G., and Calvin, D. T. (1989) Glycolaldehyde inhibits CO₂ fixation in the Cyanobacterium *Synechococcus* UTEX 625 without inhibiting the accumulation of inorganic carbon or the associated quenching of chlorophyll a fluorescence. *Plant Physiol.* **91**, 1044–1049
63. Takahashi, S., and Murata, N. (2005) Interruption of the Calvin cycle inhibits the repair of photosystem II from photodamage. *Biochim. Biophys. Acta* **1708**, 352–361
64. Joliot, P., Béal, D., and Joliot, A. (2004) Cyclic electron flow under saturating excitation of dark-adapted *Arabidopsis* leaves. *Biochim. Biophys. Acta* **1656**, 166–176
65. Bendall, D. S., and Manasse, R. S. (1995) Cyclic photophosphorylation and electron transport. *Biochim. Biophys. Acta* **1229**, 23–38
66. Allen, J. F. (2003) Cyclic, pseudocyclic and noncyclic photophosphorylation: new links in the chain. *Trends Plant Sci.* **8**, 15–19
67. Alric, J., Lavergne, J., and Rappaport, F. (2010) Redox and ATP control of photosynthetic cyclic electron flow in *Chlamydomonas reinhardtii* (l) aerobic conditions. *Biochim. Biophys. Acta* **1797**, 44–51
68. Johnson, X., and Alric, J. (2012) Interaction between starch breakdown, acetate assimilation, and photosynthetic cyclic electron flow in *Chlamydomonas reinhardtii*. *J. Biol. Chem.* **287**, 26445–26452
69. Melis, A., Zhang, L., Forestier, M., Ghirardi, M. L., and Seibert, M. (2000) Sustained photobiological hydrogen gas production upon reversible inactivation of oxygen evolution in the green alga *Chlamydomonas reinhardtii*. *Plant Physiol.* **122**, 127–136
70. Kuchenreuther, J. M., Britt, R. D., and Swartz, J. R. (2012) New insights into [FeFe] hydrogenase activation and maturase function. *PLoS One* **7**, e45850
71. Forestier, M., King, P., Zhang, L., Posewitz, M., Schwarzer, S., Happe, T., Ghirardi, M. L., and Seibert, M. (2003) Expression of two [Fe]-hydrogenases in *Chlamydomonas reinhardtii* under anaerobic conditions. *Eur. J. Biochem.* **270**, 2750–2758
72. Subramanian, V., Dubini, A., Astling, D. P., Laurens, L. M., Old, W. M., Grossman, A. R., Posewitz, M. C., and Seibert, M. (2014) Profiling *Chlamydomonas* metabolism under dark, anoxic H₂-producing conditions using a combined proteomic, transcriptomic, and metabolomic approach. *J. Proteome Res.* **13**, 5431–5451
73. Leister, D., and Shikanai, T. (2013) Complexities and protein complexes in the antimycin A-sensitive pathway of cyclic electron flow in plants. *Front. Plant Sci.* **4**, 161
74. Joliot, P., and Joliot, A. (2005) Quantification of cyclic and linear flows in plants. *Proc. Natl. Acad. Sci. U.S.A.* **102**, 4913–4918
75. Roach, T., and Krieger-Liszka, A. (2014) Regulation of photosynthetic electron transport and photoinhibition. *Curr. Protein Pept. Sci.* **15**, 351–362
76. Miyake, C. (2010) Alternative electron flows (water-water cycle and cyclic electron flow around PSI) in photosynthesis: molecular mechanisms and physiological functions. *Plant Cell Physiol.* **51**, 1951–1963
77. Armbruster, U., Carrillo, L. R., Venema, K., Pavlovic, L., Schmidtman, E., Kornfeld, A., Jahns, P., Berry, J. A., Kramer, D. M., and Jonikas, M. C. (2014) Ion antiport accelerates photosynthetic acclimation in fluctuating light environments. *Nat. Commun.* **5**, 5439
78. Carraretto, L., Formentin, E., Teardo, E., Checchetto, V., Tomizioli, M., Morosinotto, T., Giacometti, G. M., Finazzi, G., and Szabó, I. (2013) A thylakoid-located two-pore K⁺ channel controls photosynthetic light utilization in plants. *Science* **342**, 114–118
79. Tikkanen, M., and Aro, E. M. (2014) Integrative regulatory network of plant thylakoid energy transduction. *Trends Plant Sci.* **19**, 10–17
80. Kramer, D. M., and Evans, J. R. (2011) The importance of energy balance in improving photosynthetic productivity. *Plant Physiol.* **155**, 70–78
81. Alric, J. (2010) Cyclic electron flow around photosystem I in unicellular green algae. *Photosynth. Res.* **106**, 47–56